

Dextran as a Generally Applicable Multivalent Scaffold for Improving Immunoglobulin-Binding Affinities of Peptide and Peptidomimetic Ligands

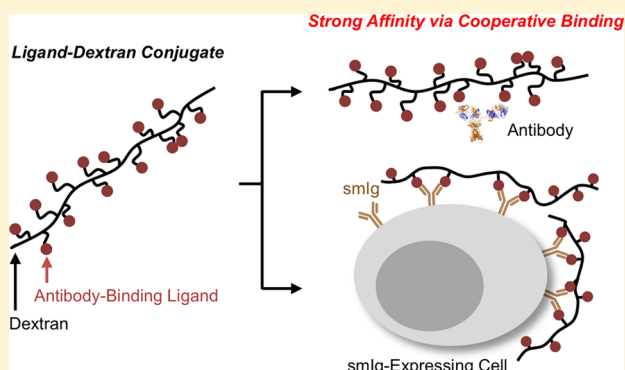
Jumpei Morimoto,[†] Mohosin Sarkar,[†] Sophia Kenrick,[‡] and Thomas Kodadek^{*,†}

[†]Departments of Chemistry and Cancer Biology, The Scripps Research Institute, 130 Scripps Way, Jupiter, Florida 33458, United States

[‡]Wyatt Technology Corporation, 6300 Hollister Avenue, Santa Barbara, California 93117-3253, United States

S Supporting Information

ABSTRACT: Molecules able to bind the antigen-binding sites of antibodies are of interest in medicine and immunology. Since most antibodies are bivalent, higher affinity recognition can be achieved through avidity effects in which a construct containing two or more copies of the ligand engages both arms of the immunoglobulin simultaneously. This can be achieved routinely by immobilizing antibody ligands at high density on solid surfaces, such as ELISA plates, but there is surprisingly little literature on scaffolds that routinely support bivalent binding of antibody ligands in solution, particularly for the important case of human IgG antibodies. Here we show that the simple strategy of linking two antigens with a polyethylene glycol (PEG) spacer long enough to span the two arms of an antibody results in higher affinity binding in some, but not all, cases. However, we found that the creation of multimeric constructs in which several antibody ligands are displayed on a dextran polymer reliably provides much higher affinity binding than is observed with the monomer in all cases tested. Since these dextran conjugates are simple to construct, they provide a general and convenient strategy to transform modest affinity antibody ligands into high affinity probes. An additional advantage is that the antibody ligands occupy only a small number of the reactive sites on the dextran, so that molecular cargo can be attached easily, creating molecules capable of delivering this cargo to cells displaying antigen-specific receptors.



■ INTRODUCTION

One of the most exciting trends in medicine over the last several years has been the development of a new generation of drugs to manipulate the immune system. For example, Rituximab, an anti-CD20 monoclonal antibody, is now employed commonly in the treatment of a variety of autoimmune diseases^{1–3} and B cell cancers.⁴ CD20 is a B cell-restricted receptor. Rituximab is thus a highly selective binding agent for all B cells that recruits effector functions of the immune system, resulting in the elimination of this cell type from patients with therapeutic benefits in the disease states mentioned above. On the cellular side, Yervoy (Ipilimumab), an anti-CTLA4 antibody, has shown efficacy in some melanoma patients, even those with metastatic disease. CTLA4 is a T cell-restricted receptor that dampens down T cell-mediated immune responses.⁵ Yervoy thus agonizes the ability of the cellular immune system to attack melanoma cells in some patients.

While impressive, this new generation of drugs is limited in that they are unable to distinguish between “good” and “bad” immune responses. In the case of Rituximab, the elimination of all B cells means that the patient is highly susceptible to new

infections^{6,7} and the reactivation of previous infections,⁸ which limits its utility as a chronic treatment. Yervoy has been found clinically to induce autoimmune conditions in some patients.⁹ For some diseases, it would thus be of great interest to develop more targeted reagents capable of agonizing or antagonizing antigen-specific immune reactions. In theory, this would allow the manipulation of pathogenic immune responses without affecting the normal function of the immune system. The only obvious way to achieve this level of selectivity is to target the antigen-specific antibodies, B cell receptors, or T cell receptors that drive the disease of interest.

A good example would be chronic lymphocytic leukemia (CLL), a common blood cancer.¹⁰ In CLL patients, a single antigen-specific B cell clone is amplified relentlessly, eventually crowding out healthy B cells and forming masses in lymph nodes and other sites. This clonal amplification strongly suggests that the pathogenic B cell is responding to stimulation

Received: May 20, 2014

Revised: July 15, 2014

Published: July 30, 2014

by an autoantigen, but the identities of CLL autoantigens are unknown. CLL patients are currently treated with a combination of cytotoxic agents and anti-CD20 antibodies such as Rituximab.¹¹ After some time the same pathogenic B cell inevitably reemerges. A drug targeted specifically to the pathogenic BCR, but that would not recognize “normal” BCRs, would constitute an ideal treatment for CLL, since it is possible that such a compound could be used chronically if it does not lead to widespread immunosuppression. Thus, we have begun a program aimed at the development of drugs targeted to antigen-specific CLL BCRs.

The simplest form of such a drug would be a high affinity, high selectivity synthetic ligand for the pathogenic BCR coupled to an appropriate toxin. Selective delivery would thus result in selective toxicity. The most obvious ligand would be the antigen itself but, as mentioned above, for CLL and, indeed, a number of important diseases, the native autoantigen is unknown. Thus, we have been interested in the development of “antigen surrogates”; synthetic unnatural compounds that can recognize the antigen-binding sites of antibodies, BCRs, or TCRs with good affinity and selectivity.^{12–14} That this is feasible was shown clearly by early experiments in which phage display or other peptide library screening techniques were employed to identify ligands for antibodies that natively bind carbohydrate epitopes.^{15–17} Indeed, peptide ligands to a few CLL BCRs have been reported.¹⁸ However, peptides have many well-known pharmacological drawbacks and we were interested instead in the development of nonpeptidic, serum stable antigen surrogates. As a first generation solution to this problem, we have reported screening protocols that allow the discovery of antibody- and TCR-binding peptoids (oligomers of *N*-substituted glycine).^{12,13,19} More recently, second generation antigen surrogates,¹⁴ and specifically ligands for CLL BCRs (M.S., J.M., and T.K., submitted), have been obtained by screening libraries of conformationally restricted oligomers, which bind proteins more tightly than the “floppy” peptoids.^{20,21} All of these molecules are highly peptidase-resistant.

The affinities of primary screening hits are typically modest especially for cases like the discovery of antigen surrogates in which there are no structural data to guide library design. While optimization efforts will undoubtedly lead to more potent derivatives, we were interested in asking if higher affinity could be achieved more quickly in the case of antibody/BCR-targeted molecules through the use of avidity effects, that is, the construction of dimers that would engage both arms of the bivalent immunoglobulin target simultaneously. While avidity effects have been used extensively to good effect in many areas of chemical biology, especially recognition of cell surface molecules,²² there is surprisingly little literature on this topic for antibody ligand development. Schweitzer-Stenner and co-workers showed that dinitrophenol (DNP) units connected by long oligoproline linkers can associate with two antigen-binding sites of a single antibody, though the affinity of this dimer for the antibody was only modestly increased over that of the monomer.²³ Baird and co-workers showed that dimers of DNP connected with long polyethylene glycol (PEG) spacers can cooperatively associate with two antigen-binding sites of anti-DNP IgE.²⁴ The best PEG-linked dimer was about 100-fold more potent than the monomer in a cellular degranulation assay that monitors the inhibition of clustering of IgE-FcεR1 receptor complexes on mast cells. Though this level of binding enhancement is still far less than what one would expect from

an ideal linker that supported full cooperativity,²⁵ it is the best reported in the literature so far for antibodies or other dimeric proteins and was attractive to us as a strategy for achieving higher affinity with our antibody ligands. However, the PEG-linked dimers have only been studied carefully in the single case of the DNP-anti-DNP IgE complex to the best of our knowledge. As we are interested in developing high-affinity peptide or peptidomimetic ligands particularly against IgG and IgM antibodies or BCRs, we considered it important to first evaluate the generality of these published observations.

We describe here the construction of various antigen-PEG-antigen dimers and test their affinities for different antibodies, including human IgG molecules (Figure 1a). To our surprise, the increase in affinity upon dimerization was not general, with some antigen-PEG-antigen molecules showing little enhancement over the monomer. However, as described below, we found that when all of the ligands tested in this study are coupled to a dextran polymer, this multivalent display universally provided a large boost in affinity for the antibody (Figure 1b). We further demonstrate here that this boost in affinity allows the detection of antigen surrogate–antibody interactions on the surface of cells by flow cytometry in a model system for the recognition of antigen-specific B cells (Figure 1c).

RESULTS AND DISCUSSION

Antigen Dimerization with PEG Linkers Does Not Reliably Lead to High Affinity Ligands. As Baird and co-workers reported, linkage of two DNP molecules with long PEG chains of a particular length supports cooperative binding to IgE antibodies.^{24,26} To probe the generality of this observation, and particularly its applicability to IgG antibodies, we first conducted an experiment on a well-characterized antigen–antibody pair: FLAG peptide (DYKDDDDK) and anti-FLAG mouse IgG1.

To create PEG-linked dimers of FLAG peptide, the copper(I)-catalyzed azide–alkyne cycloaddition (CuAAC) was employed.²⁷ First, FLAG peptide with an alkyne group at its *N*-terminus (**6**; chemical structures of all the synthesized peptides and peptoids are shown in Supporting Information Figure S1) was synthesized using the standard solid-phase method, released from the beads, and purified by HPLC. It was then coupled to bis-azide-terminated PEGs with average molecular weights of 2000 or 5000 (PEG₂₀₀₀ or PEG₅₀₀₀) using a copper catalyst (Figure 2a). The extended lengths of PEG₂₀₀₀ and PEG₅₀₀₀ were previously estimated to be 17 and 43 nm, respectively.²⁴ This should be long enough to bridge the space between the two antigen-binding sites of an IgG antibody,^{25,28,29} which is between 5.5 and 18.5 nm. The FLAG peptide-capped PEG₂₀₀₀ or PEG₅₀₀₀ dimers (**6**-PEG₂₀₀₀ or **6**-PEG₅₀₀₀) were purified by HPLC and characterized by MALDI TOF-MS (Supporting Information Figures S2 and S3). Similar dimers, but capped with the HA (influenza hemagglutinin) peptide (YPYDVPDYA) (**7**-PEG₂₀₀₀ or **7**-PEG₅₀₀₀), were synthesized in the same way as controls.

The binding affinities of these dimeric conjugates were evaluated by competition ELISA (enzyme-linked immunosorbent assay). First, a maleimide-activated 384-well ELISA plate was incubated with FLAG peptide containing a *N*-terminal cysteine residue (CSGDYKDDDDK, **1**) to immobilize FLAG peptide on the ELISA plate. Anti-FLAG mouse IgG1 was preincubated with various concentrations of (1) monomeric FLAG peptide (SGDYKDDDDK, **11**), (2) monomeric HA

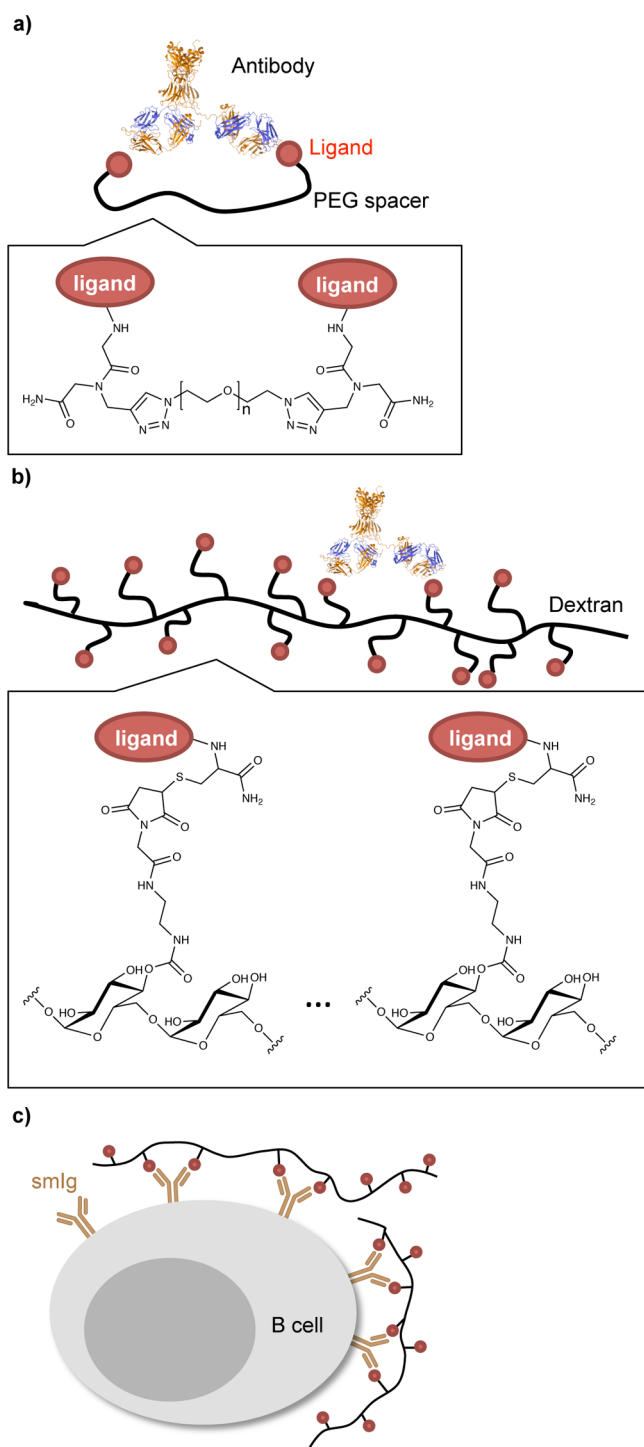


Figure 1. Schematic illustration of the interactions between antibodies and multivalent ligands. (a) An antibody and a ligand-dimer with a PEG spacer. The structure of the antibody was generated using a PDB file (1HZH). The structure of the dimer is shown in the box. (b) An antibody and a multivalent ligand on a dextran scaffold. The structure of the multivalent ligand is shown in the box. (c) Surface membrane immunoglobulin (smIg) on a B cell and multivalent ligands.

peptide (SGYPYDVPDYA, 12), (3) dimeric FLAG (6-PEG₂₀₀₀, 6-PEG₅₀₀₀), or (4) dimeric HA (7-PEG₂₀₀₀, or 7-PEG₅₀₀₀). The solutions were then applied to the FLAG-coated plate. In each well of the plate, soluble peptide monomers or dimers compete with the immobilized FLAG for binding to the anti-FLAG antibody. Therefore, by detecting the anti-FLAG antibodies

bound on the plate, binding affinities of soluble peptide monomers or dimers can be estimated indirectly. After incubation for 2 h, the wells were washed, incubated with HRP-conjugated secondary antibody, and, after another washing, treated with HRP substrate. Chemiluminescent signals from each well were detected and the data were analyzed by fitting in inhibitory curve using a nonlinear regression method. To compare the binding affinity of monomers and dimers, the *x*-axis on the plot was normalized to concentrations of monovalent peptide. In other words, the molar concentration of a dimeric construct would be half of what is plotted. Half-inhibitory concentrations (IC₅₀) were calculated from the curves (Figure 3a and b and Table 1). HA monomer and HA dimers did not compete at all up to 500 μM (Figure 3b), as expected. Surprisingly, FLAG-monomer and dimers showed similar IC₅₀ values (~10 μM), indicating that dimerization did not result in more favorable binding properties to the bivalent antibody. We also constructed an even longer PEG₁₀₀₀₀-spaced FLAG dimer, but even this construct failed to show significantly greater affinity for anti-FLAG antibody than did the monomer (Supporting Information Figure S4).

To determine if this unexpected result was peculiar to the anti-FLAG antibody-FLAG peptide complex, the analysis was repeated with two other small molecule-antibody complexes that were available from our previous work, NMOP6 peptoid and antiaquaporin 4 (AQP4) human IgG1, and ADP3 peptoid and anti-ADP3 chicken IgY. NMOP6 (Neuromyelitis optica peptoid 6) is a peptoid isolated from one of our previous serum screens and was shown previously to be a modest affinity ligand for anti-AQP4 autoantibodies.^{13,30–32} ADP3 is a peptoid found to bind to antibodies present in the serum of some patients with Alzheimer's disease.¹² In order to have a high affinity peptoid-antibody complex of utility in optimizing the conditions for the development of certain assays, we immunized chickens with this peptoid, resulting in the production of anti-ADP3 IgY antibodies.³³ Thus, the NMOP6-IgG and ADP3-IgY pairs constitute models for low and high affinity small molecule-antibody complexes, respectively.

NMOP6 and ADP3 containing an alkyne group at their *N*-terminus (8 and 10, respectively, Supporting Information) were synthesized as described above (Figure 2a) and these molecules were dimerized using the bis-azide functionalized PEGs by CuAAC to produce 8-PEG₂₀₀₀, 8-PEG₅₀₀₀, 10-PEG₂₀₀₀, and 10-PEG₅₀₀₀. Another peptoid, 9, that does not bind to either antibody was subjected to the same synthetic protocol to prepare 9-PEG₂₀₀₀ and 9-PEG₅₀₀₀, which were employed as controls for binding experiment of NMOP6 to anti-AQP4 human IgG1. For binding experiment of ADP3 to anti-ADP3 chicken IgY, NMOP6 monomer and dimers were employed as controls. The binding affinity of each ligand was evaluated by competition ELISA, as described above.

In contrast to the result obtained for the FLAG dimers, the PEG dimers of NMOP6 and ADP3 both showed much stronger competitive activities than the monomers. The IC₅₀ value of the PEG₂₀₀₀ dimer of NMOP6 (8-PEG₂₀₀₀) was 1.4 ± 0.7 μM, a value that is about 190-fold lower than that of monomeric NMOP6 (IC₅₀ 273 ± 40 μM). The PEG₅₀₀₀ dimer of NMOP6 (8-PEG₅₀₀₀) exhibited an IC₅₀ of 20.8 ± 1.0 μM, higher than that of 8-PEG₂₀₀₀, but still about 13-fold lower than that of monomeric NMOP6 (Figure 3c and d, and Table 1). Probably PEG₂₀₀₀ is a long enough spacer for this ligand-antibody pair for cooperative binding, and extension of the

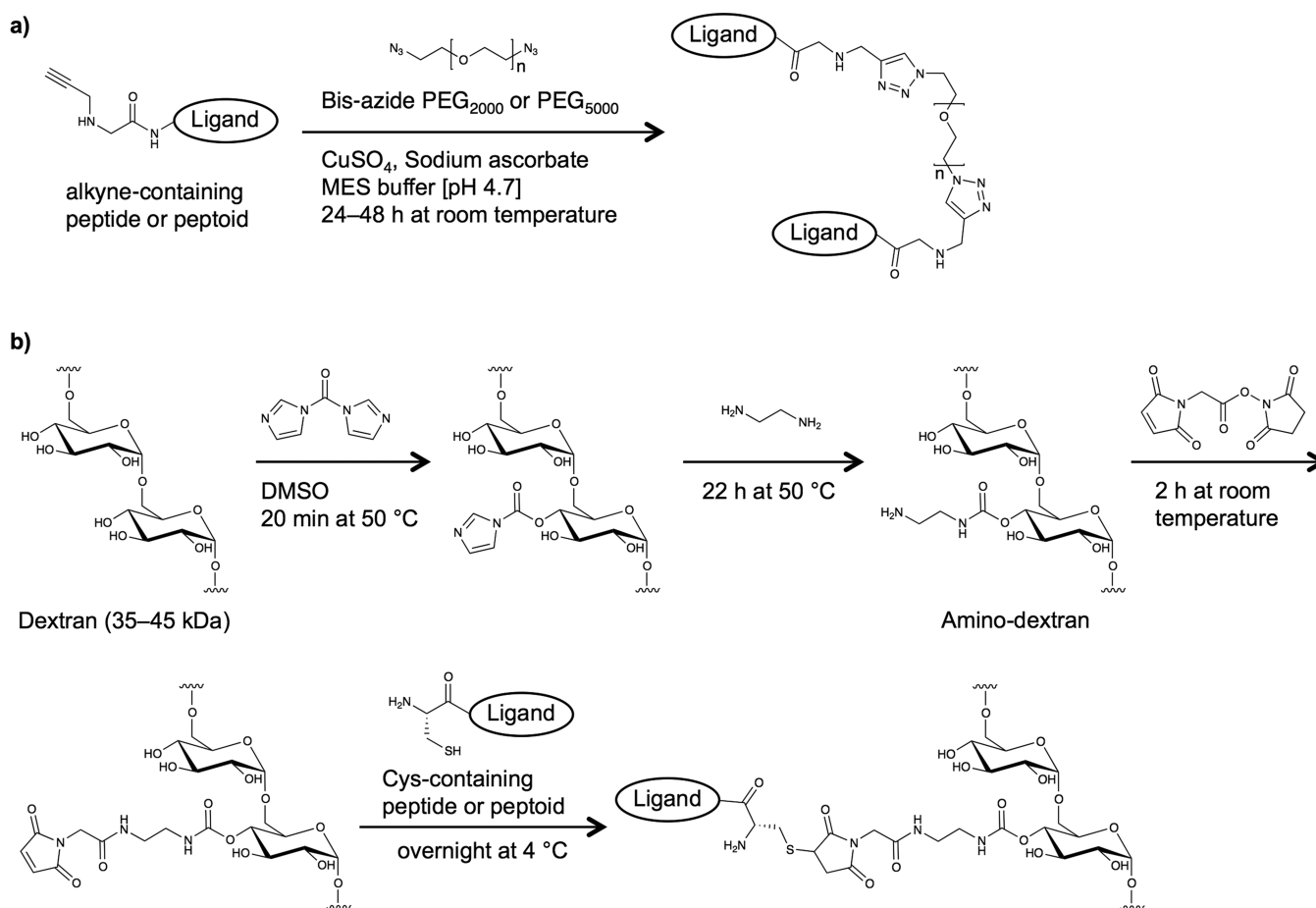


Figure 2. Synthetic schemes of (a) bivalent ligand with a PEG spacer and (b) multivalent ligand on dextran.

spacer length makes the cooperative binding less favorable because of an entropic loss.

In the case of the ADP3-containing constructs, both the PEG₂₀₀₀ dimer and PEG₅₀₀₀ dimers displayed IC₅₀ values about 600-fold lower (3.3 ± 0.1 nM and 3.3 ± 0.2 nM, respectively) than that of peptoid monomer (2.0 ± 0.7 μ M) (Figure 3e and f, and Table 1). In both cases, none of control monomers and dimers competed significantly with the immobilized ligand for antibody binding.

Taken together, these results support the idea that dimeric ligands can cooperatively bind the two antigen-binding sites of an antibody, resulting in significant improvement of binding affinity between ligand and antibody. However, as seen in these three model experiments, the degree of improvement can vary widely depending on the length of the PEG spacer and, especially, on the particular antigen–antibody interaction.

Construction of Dextran-Displayed Multivalent Ligands and Evaluation of Their Affinities against Corresponding Antibodies. Since antigen dimerization with PEG spacers will not serve as a general solution to achieving high affinity antibody binding, we turned to a different strategy in which the ligands are displayed as oligomers rather than discrete dimers. Dextran was chosen as the first scaffold to explore since it is highly water-soluble and is easy to functionalize. Also, its low nonspecific binding to proteins and low immunogenicity are advantageous over protein scaffolds such as BSA. Among various commercially available dextran products, dextran of molecular weight 35 000–45 000 (“40 kDa dextran” containing, on average, 246

glucose units) produced by *Leuconostoc mesenteroides* was used because it has a relatively small number of 1,3 glycosidic linkages (~5%) that serve as branching points.³⁴

To create the desired conjugates, a two-step protocol was employed that resulted in the modification of some of the hydroxyl groups so as to provide maleimide units suitable for attachment of ligands bearing a terminal cysteine (Figure 2). Specifically, the dextran was first treated with carbon-diimidazole, followed by ethylene diamine, to provide primary amine groups.³⁵ A colorimetric test using 2,4,6-trinitrobenzenesulfonic acid (TNBS)³⁵ showed introduction of ~43 amines per 40 kDa dextran. This amine-displaying dextran (amino-dextran) was then coupled to *N*-(α -maleimidoacetoxy)-succinimide ester (AMAS) to introduce the desired maleimide functionality. The maleimide-functionalized dextran was then incubated with cysteine-containing peptide or peptoid (1–5) to produce dextran conjugates of peptides or peptoids (Figure 2). Finally, unreacted maleimide units were quenched by incubating the conjugates with cysteine. The average number of ligands conjugated on to the dextran chain, determined from UV absorbance at 280 nm, was 14 (1), 13 (2), 13 (3), 25 (4), or 14 (5) (Supporting Information Table S1). On average, a 40 kDa dextran chain is composed of 246 1,6-linked glucose units. Since the length of a 1,6-linked glucose unit is about 4.5 Å,³⁶ the average spacing between two ligands in these dextran conjugates should be 4.4–8.5 nm, which would accommodate cooperative binding to an antibody.

The affinities of these multivalent ligands were evaluated by competition ELISAs (Figure 3 and Table 1). To compare the

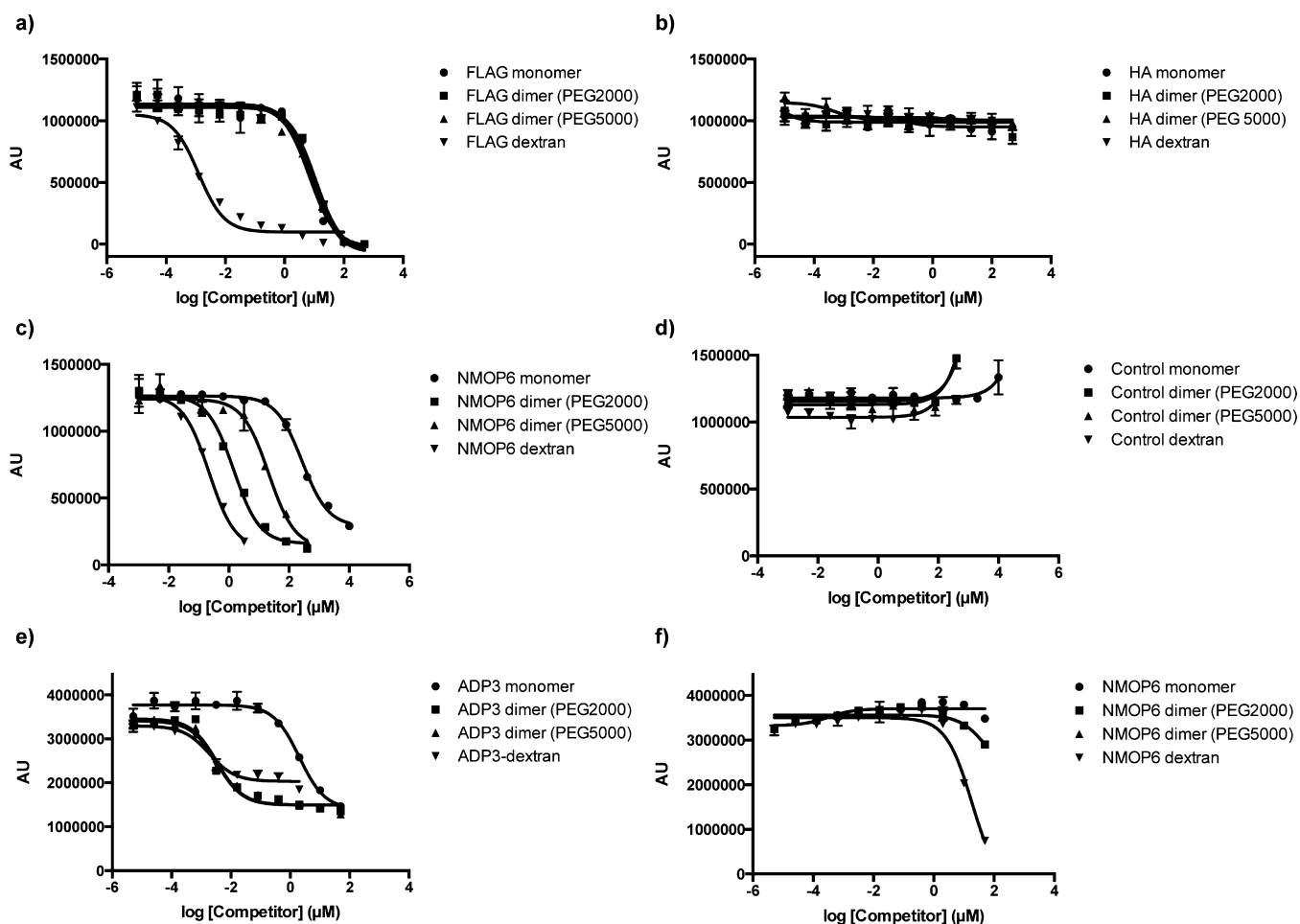


Figure 3. Determination of half-inhibitory concentrations (IC_{50} 's) of monovalent and bivalent FLAG peptides by competition ELISA. Soluble ligand–monomer, ligand–dimer with PEG₂₀₀₀ spacer, ligand–dimer with PEG₅₀₀₀ spacer, and ligand–dextran were used as competitors against interactions between immobilized ligands and antibodies. Each experiment was performed in triplicate. Average values of the triplicate runs are plotted and shown in the figure. The inhibitory curves were generated using a nonlinear regression method. The error bars represent the standard deviation. Note that the x-axis of every graph is not concentration of multivalent-ligands but of peptide or peptoid concentration on each scaffold. (a) Competition of monovalent or multivalent FLAG against the interaction between FLAG and anti-FLAG mouse IgG1. (b) Competition of monovalent or multivalent HA (influenza hemagglutinin) peptides against the interaction between FLAG and anti-FLAG mouse IgG1. (c) Competition of monovalent or multivalent NMOP6 against the interaction between NMOP6 and anti-AQP4 human IgG1. (d) Competition of monovalent or multivalent control peptide against the interaction between NMOP6 and anti-AQP4 human IgG1. (e) Competition of monovalent or multivalent ADP3 against the interaction between ADP3 and anti-ADP3 chicken IgY. (f) Competition of monovalent or multivalent NMOP6 against the interaction between ADP3 and anti-ADP3 chicken IgY.

Table 1. IC_{50} Values (nM) of Monovalent and Multivalent Ligands in Competition ELISA Experiments^a

	FLAG against anti-FLAG mouse IgG	NMOP6 against anti-AQP4 human IgG	ADP3 against anti-ADP3 chicken IgY
Monomer	8640 ± 1280	273 000 ± 40 000	2010 ± 720
Dimer (PEG ₂₀₀₀)	11 100 ± 600	1430 ± 710	3.3 ± 0.1
Dimer (PEG ₅₀₀₀)	6810 ± 200	20 800 ± 1000	3.3 ± 0.2
Multivalent (Dextran)	5.9 ± 1.1	219 ± 40.	1.9 ± 0.5

^aShown are average values and standard deviations of the triplicate of competition ELISA shown in Figure 3.

binding affinity of monomers and dextran-conjugates, the x -axis on the plot was normalized to concentrations of monovalent ligand. All three ligand–dextran conjugates, i.e., 1-dextran, 3-dextran, and 5-dextran, showed greater than 1000-fold stronger

inhibitory activity than the corresponding monomers (Figure 3a,c,e, and Table 1). The control peptide or peptoid–dextran conjugates, on the other hand, did not compete significantly in the concentration range examined (Figure 3b,d,f).

The experiment above using NMOP6 employed a patient-derived monoclonal antibody.³² It was also of interest to repeat this experiment with NMO patient serum, in which case the binding would be between the peptoid and a polyclonal family of anti-AQP4 antibodies. For this purpose sera from three healthy control individuals and three NMO patients were first tested on ELISA using an NMOP6-coated plate. Two of the three sera of NMO patients showed higher signals than the three normal sera (Supporting Information Figure S5); therefore, these two sera were regarded as samples containing anti-AQP4 antibodies that bind NMOP6. Binding affinities of NMOP6-monomer and NMOP6-dextran were evaluated using these sera by competition ELISA. An ELISA plate was coated with NMOP6, then incubated with NMO serum that was premixed with either 2 μM or 2 mM NMOP6 monomer (13)

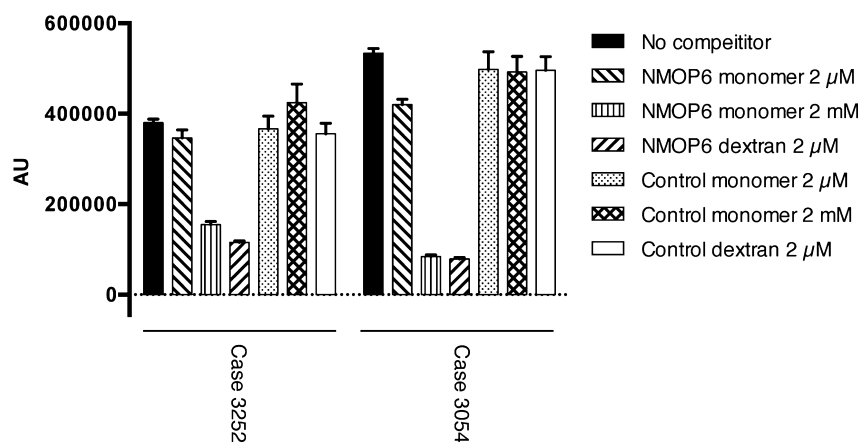


Figure 4. Competition ELISA of NMOP6 monomer, NMOP6-dextran, control monomer, and control-dextran against the interaction between immobilized NMOP6 and serum from NMO patients. Monovalent NMOP6 ($2 \mu\text{M}$ or 2mM) or multivalent NMOP6-dextran ($2 \mu\text{M}$) was mixed with a diluted serum of $200 \mu\text{g}/\text{mL}$ of total protein. Two sera from NMO patients (Cases 3252 and 3054) were tested. Each experiment was performed in triplicate and the error bars represent the standard deviation.

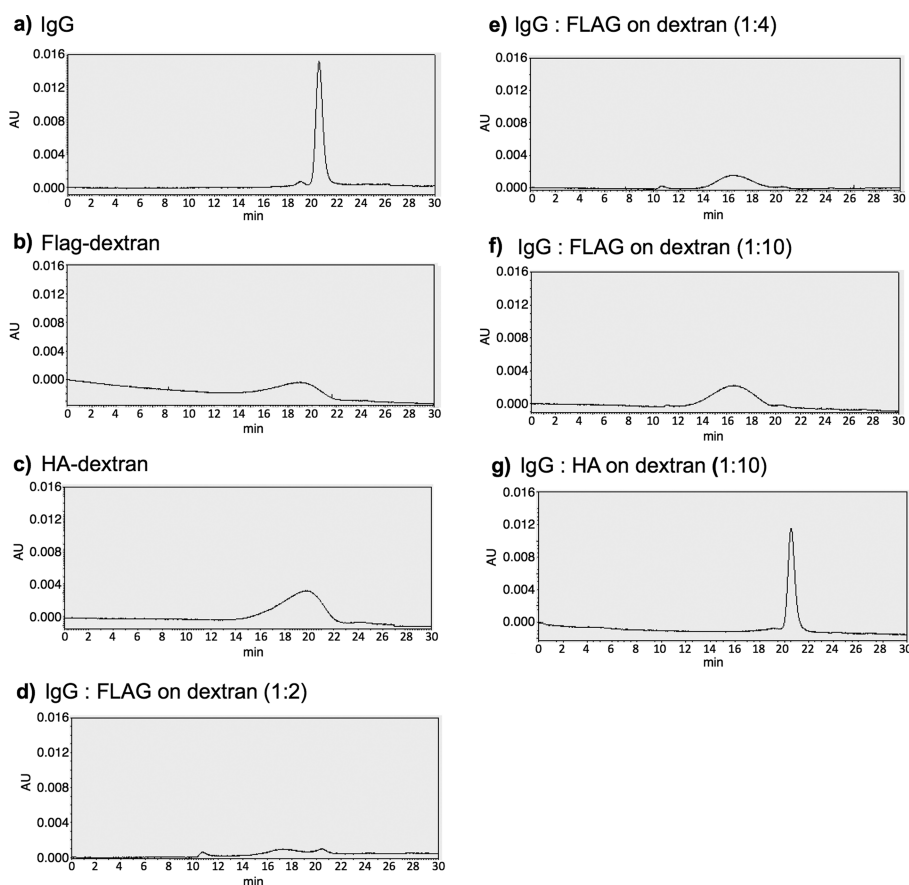


Figure 5. Size-exclusion HPLC (SE-HPLC) analysis of anti-FLAG mouse IgG1, dextran-conjugates, and anti-FLAG mouse IgG1 mixed with FLAG-dextran or HA-dextran: (a) $0.5 \mu\text{M}$ anti-FLAG mouse IgG1; (b) $5 \mu\text{M}$ FLAG-dextran; (c) $5 \mu\text{M}$ HA-dextran; (d–f) $0.5 \mu\text{M}$ anti-FLAG mouse IgG1 mixed with (d) $1 \mu\text{M}$, (e) $2 \mu\text{M}$, or (f) $5 \mu\text{M}$ FLAG conjugated on dextran. (h) $0.5 \mu\text{M}$ anti-FLAG mouse IgG1 mixed with $5 \mu\text{M}$ HA conjugated on dextran.

or $2 \mu\text{M}$ NMOP6-dextran (3-dextran). 14 and 4-dextran were used as control monomeric and multimeric competitors. As AQP4-reactive IgGs in NMO patients are predominantly IgG1, anti-IgG1 antibody conjugated with HRP was used as the secondary antibody. Signals of both sera competed well by $2 \mu\text{M}$ NMOP6-dextran (3-dextran) (Figure 4). On the other hand, NMOP6 monomer did not show much competition at 2

μM and, even at 2mM , the degree of competition was slightly poorer than that of the dextran conjugate. In other words, $2 \mu\text{M}$ dextran conjugate competes better than 2mM monomer. This indicates that over a 1000-fold improvement in the binding affinity was achieved by dextran conjugation, which is a similar degree of improvement that was observed with the monoclonal anti-AQP4 antibody.

These data show that ligands displayed on dextran bind about 3 orders of magnitude more strongly than monomers regardless of the nature of the ligand and antibody, at least for the three cases studied. This is in clear contrast with the results obtained for the PEG-linked dimers. Thus, dextran conjugation can be considered a generally applicable strategy to improve the affinity of an antibody ligand.

Characterization of the Complex Formed between FLAG-Dextran and anti-FLAG IgG1. To probe the nature of the complexes that are formed between the antibody and the ligand–dextran conjugates, the association of anti-FLAG mouse IgG1 and FLAG-dextran (1-dextran) was analyzed by size exclusion HPLC (SE-HPLC). When IgG and 1-dextran were injected to the size exclusion column individually, the IgG eluted at 20–21 min (Figure 5a) and 1-dextran eluted between 16 and 22 min (Figure 5b). Upon addition of 2 equiv of FLAG peptide conjugated on dextran to the IgG, a new broad peak appeared at 13–20 min on the chromatogram and the IgG peak at 20–21 min became almost invisible (Figure 5d), suggesting that most of the IgG formed complex with 1-dextran. Because a single IgG has two antigen-binding sites, the ratio of antigen-binding sites and FLAG peptide is 1:1 in this condition. This means that there are enough ligands on dextran to saturate all the antigen-binding sites. By increasing the ratio of FLAG-dextran to IgG, the area of the peak at 20–21 min completely disappeared, and the peak at 13–20 min became more prominent (Figure 5e and f), suggesting that all of the IgG binds to 1-dextran in this ratio. As a control, we also mixed anti-FLAG mouse IgG1 with 2-dextran and analyzed by SE-HPLC. (A chromatogram of 2-dextran alone is shown in Figure 5c.) The elution time and area of IgG were unaffected by this conjugate (Figure 5g), demonstrating that the complex formation between 1-dextran and anti-FLAG mouse IgG1 is selective.

Binding of the anti-FLAG IgG to FLAG-dextran was also examined by native polyacrylamide gel electrophoresis (native PAGE). The complex formation between FLAG-dextran and anti-FLAG IgG antibody was observed as the mobility shift of antibody upon addition of FLAG-dextran (Supporting Information Figure S6a). No such shift was observed upon mixing the antibody with HA-dextran (Supporting Information Figure S6b). This data also support the selective formation of a complex between 1-dextran and anti-FLAG mouse IgG1.

To characterize the size of the complexes, they were further analyzed by size exclusion chromatography (SEC) equipped with a multiangle light scattering (MALS) detector. First, 1-dextran alone was analyzed on this system. Simultaneous concentration measurements by UV and differential refractive index (dRI) enabled the determination of the protein and dextran mass fractions, yielding the composite molar mass of the entire molecule as well as the molar mass of each component. The polydisperse 1-dextran eluted from the column at 12.5–20 min (Figure 6a purple line), and the weight-average molar mass (M_w) of this broad peak was determined to be $164\,000 \pm 300$ Da. Protein conjugate analysis revealed the FLAG peptide composed 24–29% of the molar mass of the conjugate with $M_w = 42\,900$ Da from the FLAG peptide and $M_w = 121\,000$ Da from dextran (Table 2). The measured M_w of 121 000 Da for dextran is about 3-fold higher than the molecular weight of unconjugated dextran ($\sim 40\,000$ Da). This indicates that, on average, three dextran chains were cross-linked during synthesis, most probably at the amine-functionalizing reaction step (second arrow in Figure 2b). A M_w

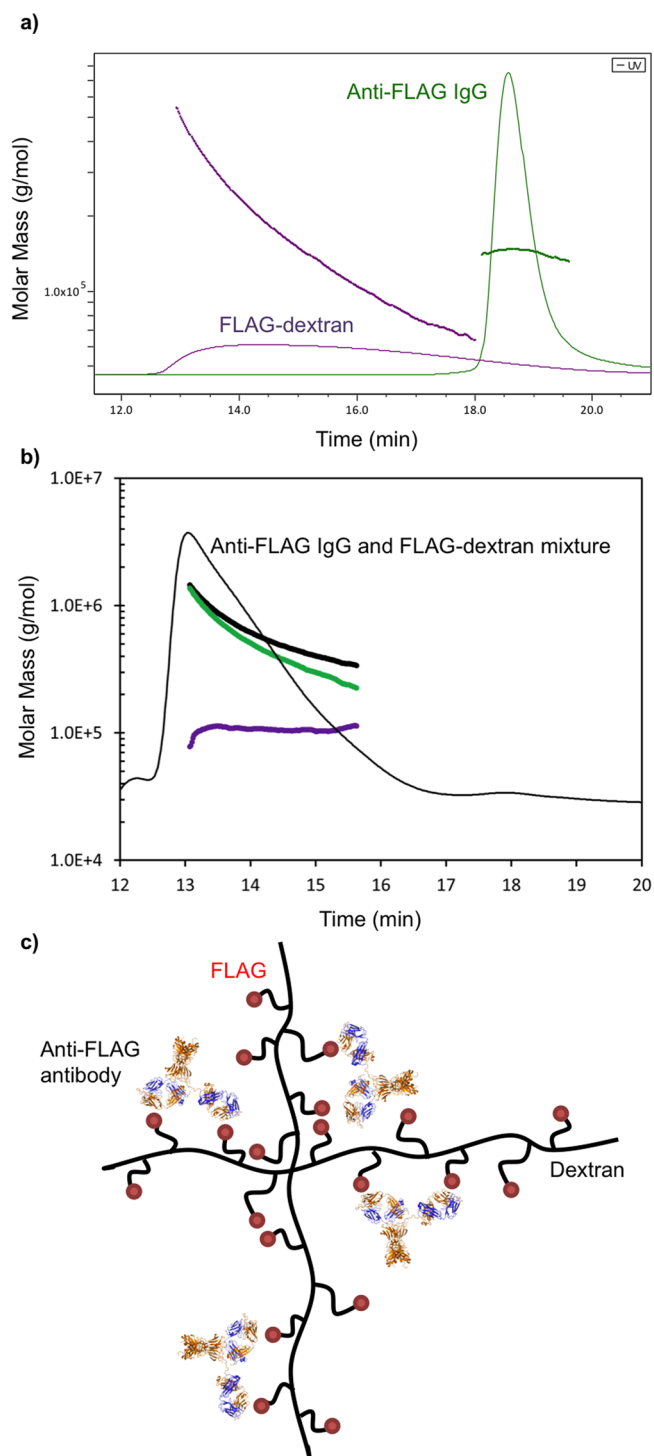


Figure 6. Size-exclusion chromatography multiangle light-scattering (SEC-MALS) analysis of (a) anti-FLAG mouse IgG1 (green) and FLAG-dextran (purple) and (b) a complex formed in a 1:10 mixture of anti-FLAG mouse IgG1 and FLAG-dextran (black). For each chromatogram, the measured molar mass (left axis) as a function of elution volume is overlaid on the UV signal. In the case of the complex formed between the anti-FLAG IgG and FLAG-dextran (b), the composite molar mass is shown in black, the contribution from the FLAG-dextran is shown in purple, and the contribution from the bound antibody is shown in green. (c) Schematic illustration of an average complex of FLAG-dextran and anti-Flag mouse IgG1.

of 42 900 Da corresponds to 34 Flag peptides and, considering 3 molecules of 40 kDa dextran are cross-linked, about 11 Flag

Table 2. Weight Average Molar Mass (M_w), Number Average Molar Mass (M_n), and Polydispersity of anti-FLAG IgG1, FLAG-Dextran, and a Complex of the Two Molecules^a

	anti-FLAG IgG1	FLAG-dextran	complex
M_w [$\times 10^{-3}$]	145 \pm 0.2	164 \pm 0.3 (FLAG 42.9 \pm 0.1) (Dextran 121 \pm 0.5)	703 \pm 0.8 (IgG 598 \pm 0.8) (FLAG-dextran 105 \pm 0.8)
M_n [$\times 10^{-3}$]	145 \pm 0.2	124 \pm 0.4	601 \pm 1.0
Polydispersity	1.00	1.32 \pm 0.01	1.17

^aThe values were determined from the SEC-MALS data in Figure 6.

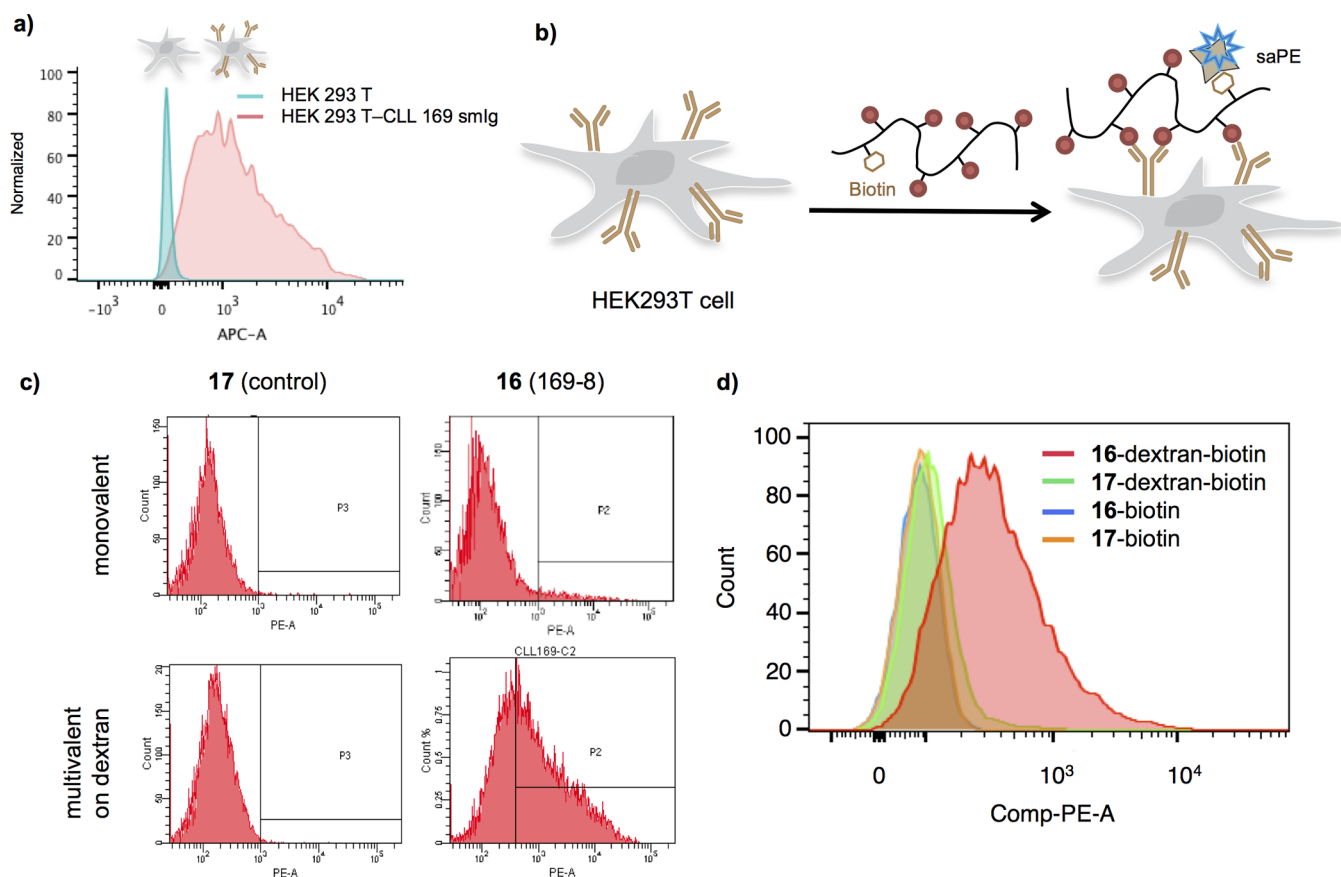


Figure 7. Cell binding assay with monovalent and multivalent ligands. (a) HEK 293 T cells were transiently cotransfected with heavy and light chain plasmid pairs (pIg-gamma and pIg-lambda) of smlg 169, and the expression levels of smlg was determined by staining cells with antihuman Fc antibody conjugated to allophycocyanin (anti-huFc-APC) and analyzing the stained cells on flow cytometry. (b) Schematic illustration of cell binding assay in which HEK 293 T cells expressing CLL smlg are treated with biotin-conjugated ligands followed by staining the cells with phycoerythrin conjugated streptavidin (saPE) and anti-huFc-APC. Cells are sorted based on APC signal for expression of CLL smlgs and on PE signal for the binding of monovalent or multivalent ligands on the cell surface. (c) FACS analysis of cells expressing smlg 169 that were stained using monovalent and multivalent ligands. (d) Overlaid FACS histograms of (c) for comparison of binding of monovalent and multivalent peptides against smlg 169 on HEK 293 T cell surface.

peptides are on each 40 kDa dextran chain, on average. This number roughly agrees with the initial number calculated from UV absorbance (Supporting Information Table S1) of 14 FLAG peptides per 40 kDa dextran.

Next, anti-FLAG mouse IgG1 was mixed with 10 mol equiv of FLAG peptide conjugated to dextran and the mixture was analyzed using the SEC-MALS system. In this experiment, based on the SEC-MALS result that about 11 FLAG peptides are on single 40 kDa dextran, the ratio of antibody and dextran molecules should be approximately 1:1. The prominent peak on the size-exclusion chromatogram appeared at 12.5–16 min. The M_w of this peak measured 703 \pm 0.8 kDa. Protein conjugate analysis revealed the 1-dextran portion of the mass had M_w of 105 000 g/mol, and the portion of the molar mass resulting from bound antibody had M_w of 598 000 Da. This

suggests that under these conditions the major complex contains \sim 4 antibodies, \sim 20 FLAG peptides, and \sim 2 molecules of 40 kDa dextran (Figure 6c).

Selective Labeling of Cells Expressing Surface Membrane Immunoglobulins of a Chronic Lymphocytic Leukemia Clone Using a Peptide–Dextran Conjugate. B cells express surface membrane immunoglobulins (smIgs), which is also known as B cell receptor (BCR), on their cell surface that have the same antigen-binding sequences as the soluble antibodies that will be produced by the corresponding plasma cells. Therefore, the dextran-conjugates of antibody ligands should also be interesting ligands for recognition of antigen-specific B cells.

To test this idea in a model system, we employed a peptide called 169-8 (DNYAAALAQRR) that has been reported by

Chiroazzi and co-workers to be a high affinity ligand for a BCR derived from a patient with CLL, designated CLL169.¹⁸ We synthesized the peptide on solid phase with an *N*-terminal cysteine residue and a GSSG spacer between the cysteine and the 169-8 sequence (**16**). The peptide was biotinylated using maleimide-functionalized biotin (**16**-biotin). To prepare a dextran conjugate of **16**, amino-dextran was first reacted with biotin-NHS to introduce a few biotin molecules on dextran, and then the residual amino groups on amino-dextran were conjugated with **16** using the AMAS linker (**16**-dextran-biotin).

Monovalent and dextran-conjugated 169-8 peptides were tested for their efficacy to recognize CLL 169 smIg expressing on Human Embryonic Kidney 293 T (HEK 293 T) cells. HEK 293 T cells expressing other nonselecting CLL BCRs with different antigen-binding sequences were used as controls. The smIg was transiently expressed in HEK 293 T cells by cotransfecting plasmids coding the light chain and heavy chain of smIg. The expression levels of smIgs were monitored by labeling the transfected cells with anti-human Fc antibody conjugated with allophycocyanin (anti huFc-APC) followed by analysis using flow cytometry (Figure 7a). The transfected cells were incubated with **16**-biotin or **16**-dextran-biotin and, after washing, further incubated with phycoerythrin-conjugated streptavidin (saPE). The cells were then analyzed by flow cytometry to detect PE signals from binding of the ligands on cells.

16-Biotin did not bind detectably to the cells expressing smIg 169 (Figure 7c right-top panel). This initially was surprising since the reported K_D of the 169-8 peptide-CLL 169 antibody complex is 31 nM³⁷ but is likely due to a relatively short half-life of the complex, which must survive time-consuming washing steps to be detected. In any case, the dextran conjugate (**16**-dextran-biotin) significantly increased the population of cells showing high PE-fluorescence (Figure 7c right-bottom panel and d), indicating the efficient binding of dextran conjugate on the cells via CLL 169 smIg. We also synthesized a control peptide (CGSSGFLAQLWSALEY, **17**), prepared its biotin conjugate (**17**-biotin) and dextran conjugate (**17**-dextran-biotin), and tested their binding to the cells expressing CLL169 smIg. Neither the monomer nor the dextran conjugate bound detectably to the cells (Figure 7c left panels), which excludes the possibility that dextran interacts nonspecifically with the transfected cells.

In order to evaluate selectivity of **16**-dextran for CLL 169 smIg, three other smIgs of CLL patient 014, 068, or 183 were also transiently expressed on HEK 293 T cells and the cells were tested for labeling by **16**-dextran and control **17**-dextran. The expression of smIgs on HEK 293 T cells were optimized to be at similar levels (Supporting Information Figure S7 bottom panels). None of these cells displaying a smIg (014, 068, or 183) with a different antigen-binding specificity were detectably stained by any of the molecules (**16**-biotin, **16**-dextran-biotin, **17**-biotin, or **17**-dextran-biotin; Supporting Information Figure S7 middle and top panels). In accord with the previous experiment, a significant population of cells expressing CLL 169 smIg was stained with PE indicating that the **16**-dextran-biotin recognized the cells expressing only CLL 169 smIg with high specificity.

These experiments demonstrate that the dextran conjugate of peptide 169-8 achieves high affinity for CLL 169 smIg without sacrificing high selectivity. It should be pointed out that **16**-dextran can interact not only with two antigen-binding sites of single CLL 169 smIg, but also with multiple CLL 169 smIg

molecules, since cells express numerous smIgs on their surface. Therefore, the affinity improvement of the ligand observed here may reflect this effect as well as the cooperative binding of ligands to two arms of the same IgG.

CONCLUSION

In this study, we sought to develop a general and reliable method to rapidly transform modest affinity antibody ligands into much higher affinity constructs by taking advantage of avidity effects. Ligand dimers with PEG spacers proved unreliable. In the three cases examined, PEG linkage improved binding affinities of ADP3 greatly against chicken IgY, improved NMOP6 binding to a human IgG1 protein modestly, and had little effect on binding of FLAG peptide to anti-FLAG antibody.

A previous study using DNA nanostructures suggested that the degree of linker flexibility can affect the stability of the complex between an antibody and a multivalent ligand significantly.³⁸ The PEG scaffold is highly flexible and each of the antibodies may have a different degree of flexibility in the hinge region, allowing the arms to “flap” to different degrees.^{29,39,40} So, the different dynamics of each system could be a contributing factor, though we cannot claim to understand in detail the underlying reason for this variability. One could make an argument for the use of more rigid bivalent compounds. Indeed, Janssen and co-workers linked two peptides that bind an anti-HIV mouse IgG1 with a relatively rigid DNA duplex to make various sizes of DNA-linked peptide dimers and showed that some of these dimers can associate cooperatively with two antigen-binding sites of anti-HIV antibodies, resulting in a greater than 500-fold improvement in binding affinity compared to the monomeric form of the peptide.⁴¹ However, until more complexes are studied it remains to be determined how generally this strategy could be applied to other antigen–antibody complexes. Moreover, the use of DNA linkers would raise concerns about serum stability, a critical issue for the development of therapeutics.

Thus, none of the published linker strategies fulfilled our requirement for a rapid and generally reliable serum-stable scaffold with which to increase the affinity of antibody ligands for the protein greatly. As shown in this study, conjugation of ligands to dextran suits this purpose nicely. In all three cases studied, an approximately 1000-fold increase in affinity of the dextran conjugate for the antibody relative to the monomer was observed. We also demonstrated that the dextran conjugates can deliver a cargo molecule (in this case biotin) to a cell displaying a membrane anchored form of the target antibody. This provides a reasonable model for the delivery of effector molecules to antigen-specific B cells and sets the stage for efforts to develop drugs and/or tool compounds capable of manipulating antigen-specific immune responses. The dextran conjugates may have advantages over other molecular formats, such as encapsulating cargo inside modified nanoparticles, such as poly(lactic-*co*-glycolic acid) (PLGA), given the smaller size of the dextran and the ease with which it can be modified synthetically.

MATERIALS AND METHODS

Chemicals. All the Fmoc-protected amino acids and Knorr Amide MBHA resin (0.75 mmol/g) were purchased from Novabiochem. All the other chemicals used for peptide and peptoid synthesis were purchased from Sigma-Aldrich, Acros

Organics, or Oakwood Chemical. Commercial sources of other chemicals used in this study are described in each experimental section.

Antibodies. Anti-FLAG M2 mouse IgG1 (F3165) was purchased from Sigma-Aldrich. Anti-AQP4 human IgG1 was obtained from Jeffrey L. Bennett (U. of Colorado). Anti-ADP3 chicken IgY was obtained by immunizing a chicken with ADP3 (Creative Biolabs). Donkey anti-mouse IgG antibody, HRP conjugate (AP192P), and donkey anti-chicken IgY antibody, HRP conjugate (AP194P) were purchased from Millipore. Mouse Anti-Human IgG1 (hinge)-HRP (clone 4E3, 9052-05) was purchased from Southern Biotech.

Buffers. Phosphate buffered saline (PBS, pH 7.4) was prepared by diluting 10× PBS (Corning, 46-013-CM) with distilled water. PBS-T was prepared by adding 0.05 v/v% of Tween-20 to PBS. MES buffered saline (MES, pH 4.7) was prepared by dissolving one pack of BupH MES Buffered Saline (Thermo Scientific, 28390) with 500 mL of distilled water.

Sera. Normal sera were obtained from three healthy individuals. The collection procedure was approved by the Scripps IRB (protocol number: IRB-13-6253). NMO patient serum samples were obtained from Dr. Michael Levy (Johns Hopkins School of Medicine) and the Accelerated Cure Project.

Peptide Synthesis. Structures of synthesized peptides are shown in Supporting Information Figure S1 (1, 2, 6, 7, 11, and 12). Each peptide was synthesized on 100 mg of Knorr Amide MBHA resin using the standard solid-phase Fmoc peptide synthetic method. For 6 and 7, after the deprotection of Fmoc on Ser, a propargyl group was introduced at their N-terminus by using the standard submonomer method for peptoid synthesis as follows. First, a DMF solution containing bromoacetic acid (20 equiv, 1M) and diisopropylcarbodiimide (10 equiv, 0.5 M) was applied to the resin and the reaction vessel was incubated at 37 °C for 10 min. After washing with DMF three times, the resin was shaken in 1 M propargylamine (20 equiv) in DMF for 1 h at 37 °C.

All the peptides were purified on HPLC using C18 reverse phase column, lyophilized, and stored at −20 °C.

Peptoid Synthesis. Structures of synthesized peptoids are shown in Supporting Information Figure S1 (3, 4, 5, 8, 9, 10, 13, 14, and 15). Each peptoid was synthesized on 100 mg of Knorr Amide MBHA resin using the standard submonomer method.⁴²

All the peptoids were purified on HPLC using C18 reverse phase column, lyophilized, and stored at −20 °C.

Synthesis of Biotinylated Peptides. 16 was synthesized with a N-terminal Mmt (monomethoxytrityl)-protected cysteine on Rink amide MBHA resin following the standard solid-phase peptide synthesis (SPPS) protocol. The Mmt group was deprotected from Cys by 1% TFA and biotin-maleimide (Sigma) was conjugated to the peptide by Michael reaction through the deprotected thiol group on Cys. The peptide was released from the resin by TFA cocktail (94% TFA, 2% thioanisole, 2% triisopropylsilane, 2% H₂O), purified on HPLC using C18 reverse phase column, lyophilized, and stored at −20 °C.

17 was purchased from Sigma-Aldrich and was conjugated to biotin by Michael reaction using biotin-maleimide (Sigma-Aldrich) in solution phase. Two molar excess of biotin-maleimide was added to the peptide in PBS [pH 7.2] and the reaction was carried out for 2 h at room temperature. Biotin conjugation was confirmed by MALDI-TOF mass spectrometry

and the biotinylated peptide was purified on HPLC using reverse phase C18 column, lyophilized, and stored at −20 °C.

Synthesis of Peptide (or Peptoid)-PEG Dimers. 840 μL of 2.6 mM alkyne-containing peptide or peptoid (6–10, 2.2 μmol) was mixed with 50 μL of 20 mM polyoxyethylene bis(azide) of molecular weight 2000 or 5000 (Sigma-Aldrich) (1 μmol), 10 μL of 100 mM CuSO₄ (Acros Organics) (1 μmol), and 100 μL of 100 mM sodium ascorbate (Spectrum Chemical) (10 μmol) in 20 mM MES (pH 4.7) buffer containing 30 mM NaCl and incubated for 24–48 h with a gentle rotation at room temperature. After the incubation, the solution was acidified by adding 20 μL of 10% trifluoroacetic acid aqueous solution and purified by HPLC.

Synthesis of Amino-Dextran. Amino-dextran was prepared as previously reported.³⁵ 500 mg of dextran (average molecular weight 35 000–45 000, from *Leuconostoc mesenteroides*, Sigma-Aldrich) was dissolved in anhydrous DMSO in 50 mL tube. The solution was warmed to 50 °C to completely dissolve the dextran. 126 mg of *N,N'*-carbonyldiimidazole in 500 μL of anhydrous DMSO was added and the solution was incubated with gentle shaking at 50 °C for 20 min. After the incubation, 250 μL of ethylenediamine was added and the solution was incubated with gentle shaking at 50 °C for 22 h. 25 mL of acetone was added and the solution was cooled on ice for 15 min. The tube was centrifuged at 700g for 10 min and the supernatant was removed. The pellet was resuspended in 20 mL of acetone and the tube was centrifuged at 700g for 10 min. The supernatant was removed and the pellet was air-dried. The dried pellet was dissolved in 10 mL of ultrapure water and the solution was dialyzed with Snakeskin dialysis tubing (7 MWCO, Thermo Scientific) for 2 days. The dialyzed dextran was lyophilized and used for peptoid/peptide conjugation. The extent of amine derivatization was determined by a colorimetric test using 2,4,6-trinitrobenzenesulfonic acid (TNBS).⁴³

Peptide/Peptoid Conjugation with Amino-Dextran. 120 μL of 100 mM *N*-(α -maleimidoacetoxy)succinimide ester (AMAS) (Thermo Scientific) in DMSO was diluted with 1 mL of PBS, and then immediately mixed with 1 mL of 6.48 mg/mL amino-dextran in PBS (40 μmol glucose units). After incubation at room temperature for 2 h in the dark, the solution was diluted with 3 mL of PBS, applied to an Amicon Ultra 4 mL centrifugal filter unit 10 000 NMWL (Millipore), and centrifuged at 2700g for 12 min. The solution in the filter unit was diluted with PBS to 4 mL and centrifuged at 2700g for 13 min. The AMAS conjugated amino-dextran solution was recovered from the filter unit then 15% (vol %) of the solution (containing 6 μmol glucose units) was mixed with 36 μL of 50 mM cysteine-containing peptide/peptoid (1–5) (1.8 μmol) in PBS and incubated at room temperature for 2 h. After the incubation, unreacted maleimide groups were quenched by adding 15 μL of 100 mM cysteine in PBS and incubating the mixture for 2 h at room temperature. After the incubation, the reaction mixture was applied to an Amicon Ultra 0.5 mL centrifugal filter unit 10 000 NMWL (Millipore) and centrifuged at 14 000g for 4 min. The concentrated solution in the filter unit was diluted with 400 μL of PBS and it was centrifuged at 14 000g for 4 min again. This washing step was repeated three more times. The ligand–dextran conjugate in the filter unit was recovered according to the manufacturer's protocol. The concentration of peptoid/peptide on each polymer was calculated from UV absorbance at 280 nm using $\epsilon_{280} = 1280$ for a tyrosine residue in peptide and $\epsilon_{280} = 3000$ for

a Npip residue, $\epsilon_{280} = 1350$ for a Ntyr residue, and $\epsilon_{280} = 60$ for a Nffa residue in peptoids.

Preparation of 169-8-Dextran Containing Biotins. 3 μL of 100 mM biotin-NHS (Thermo Scientific) was diluted with 500 μL of PBS and then immediately mixed with 500 μL of 6.48 mg/mL amino-dextran in PBS (40 μmol glucose units). The mixture was incubated at 4 °C overnight. After the incubation, 60 μL of 100 mM *N*-(α -maleimidoacetoxy)-succinimide ester (AMAS) (Thermo scientific) in DMSO was added and the mixture was incubated at RT for 2 h in the dark. The solution was diluted with 3 mL of PBS, applied to an Amicon Ultra 4 mL centrifugal filter unit 10 000 NMWL (Millipore), and centrifuged at 2700g for 12 min. The solution in the filter unit was diluted with PBS to 4 mL and centrifuged at 2700g for 13 min. The AMAS conjugated amino-dextran solution (~500 μL) was recovered from the filter unit and diluted 10-fold with PBS (5 mL). 4 μL of the solution (containing ~16 nmol glucose units) was mixed with 100 μL of 50 μM cysteine-containing peptide (16 or 17) (5 nmol) in PBS and 2 μL of 500 mM EDTA in PBS and incubated at 4 °C overnight. After the incubation, unreacted maleimide groups were quenched by adding 1 μL of 10 mM cysteine in PBS and incubating the mixture for 2 h at room temperature. After the incubation, the reaction mixture was applied to an Amicon Ultra 0.5 mL centrifugal filter unit 10 000 NMWL (Millipore) and centrifuged at 14 000g for 4 min. The concentrated solution in the filter unit was diluted with 400 μL of PBS and it was centrifuged at 14 000g for 4 min again. This washing step was repeated three more times. The ligand–dextran conjugate in the filter unit was recovered according to the manufacturer's protocol. The concentration of biotin in the solution was determined using Fluorescence Biotin Quantification Kit (Thermo Scientific).

Competition Assay on ELISA. A 384-well maleimide activated plate (Thermo Scientific) was washed with 50 μL of PBS-T three times and incubated with 20 μL of 20 μM cysteine-containing peptide/peptoid (1–5) in PBS containing 10 mM ethylenediaminetetraacetic acid (EDTA) overnight at 4 °C in the dark with gentle shaking. After washing with 50 μL of PBS-T three times, residual maleimide groups on the plate was blocked by incubating with 50 μL of 10 $\mu\text{g}/\text{mL}$ L-cysteine hydrochloride monohydrate (Thermo Scientific) for 1 h at room temperature with gentle shaking. During incubation, the competitors (monomers, dimers with PEG₂₀₀₀ or PEG₅₀₀₀, or dextran conjugates) were serially diluted with PBS-T and 35 μL of each of serial dilution series was mixed with 35 μL of antibody solution (50 pM anti-FLAG M2 mouse IgG1, 40 nM anti-AQP4 human IgG1, or 100 nM anti-ADP3 chicken IgY) in 2 \times blocking buffer. The 2 \times blocking buffer is either StartingBlock (PBS) Blocking Buffer (Thermo Scientific) containing 2% BSA (for anti-FLAG mouse IgG1 and anti-AQP4 human IgG1) or StartingBlock (PBS) Blocking Buffer (Thermo Scientific) containing 4% BSA (for anti-ADP3 chicken IgY). These competitor–antibody mixtures were incubated at room temperature until the next blocking step was done. After the incubation with the cysteine solution, the plate was washed with 50 μL of PBS-T three times and blocked with 50 μL of 1 \times blocking buffer (prepared by diluting 2 \times blocking buffer with an equal volume of PBS-T) for 1 h at room temperature with gentle shaking. After removing the blocking buffer from the plate, 20 μL of the preincubated competitor–antibody mixture was applied to each well and the plate was incubated at room temperature for 2 h with gentle shaking.

After washing with 50 μL of PBS-T three times, 20 μL of horseradish peroxidase (HRP)-conjugated secondary antibody (1/20 000 donkey anti-mouse IgG antibody for anti-FLAG mouse IgG1, and 1/2000 goat anti-human IgG antibody for anti-AQP4 human IgG1, or 1/40 000 donkey anti-chicken IgY antibody for anti-ADP3 chicken IgY) in 1 \times blocking buffer was added to each well and the plate was incubated at room temperature for 1 h with gentle shaking. After washing with 50 μL of PBS-T three times, chemiluminescence signal was developed by incubating each well with 20 μL of SuperSignal ELISA Pico Chemiluminescent Substrate (Thermo Scientific) at room temperature for 1 min with gentle shaking, and the luminescent signal was recorded on a Infinite M1000 PRO instrument (Tecan).

ELISA of Serum Samples Obtained from Healthy Individuals and NMO Patients. A 384-well maleimide activated plate was washed with 50 μL of PBS-T three times and incubated with 20 μL of 20 μM cysteine-containing NMOP6 (3) in PBS containing 10 mM EDTA for overnight at 4 °C in the dark with gentle shaking. After washing with 50 μL of PBS-T three times, residual maleimide groups on the plate was blocked by incubating with 50 μL of 10 $\mu\text{g}/\text{mL}$ L-cysteine hydrochloride monohydrate for 1 h at room temperature with gentle shaking. After the incubation, the plate was washed with 50 μL of PBS-T three times and blocked with 50 μL of blocking buffer (PBS-T containing 1 v/v% BSA) for 1 h at room temperature with gentle shaking. After removing the blocking buffer from the plate, 20 μL of serum of 200 $\mu\text{g}/\text{mL}$ total protein in blocking buffer was applied to each well and the plate was incubated at room temperature for 2 h with gentle shaking. After washing with 50 μL of PBS-T three times, 20 μL of 1/2000 goat anti-human IgG, HRP conjugated, in 1 \times blocking buffer was added to each well and the plate was incubated at room temperature for 1 h with gentle shaking. After washing with 50 μL of PBS-T three times, chemiluminescence signal was developed by incubating each well with 20 μL of SuperSignal ELISA Pico Chemiluminescent Substrate at room temperature for 1 min with gentle shaking and the luminescent signal was recorded on a Infinite M1000 PRO instrument.

Competition Assay on ELISA of Serum Samples Obtained from NMO Patients. A 384-well maleimide activated plate was washed with 50 μL of PBS-T three times and incubated with 20 μL of 20 μM cysteine-containing NMOP6 (3) in PBS containing 10 mM EDTA for overnight at 4 °C in the dark with gentle shaking. After washing with 50 μL of PBS-T three times, residual maleimide groups on the plate was blocked by incubating with 50 μL of 10 $\mu\text{g}/\text{mL}$ L-cysteine hydrochloride monohydrate for 1 h at room temperature with gentle shaking. During the incubation, the competitors (monomers, dimers with PEG₂₀₀₀ or PEG₅₀₀₀, or dextran conjugates) were serially diluted with PBS-T and 35 μL of each of serial dilution series was mixed with 35 μL of serum of 400 $\mu\text{g}/\text{mL}$ total protein in 2 \times blocking buffer (PBS-T containing 2% BSA). These competitor–antibody mixtures were incubated at room temperature until the next blocking step is done. After the incubation with the cysteine solution, the plate was washed with 50 μL of PBS-T three times and blocked with 50 μL of 1 \times blocking buffer (prepared by diluting 2 \times blocking buffer with an equal volume of PBS-T) for 1 h at room temperature with gentle shaking. After removing the blocking buffer from the plate, 20 μL of the preincubated competitor–antibody mixture was applied to each well and the plate was incubated at room temperature for 2 h with gentle shaking. After washing with 50

μL of PBS-T three times, 20 μL of 1/2000 goat antihuman IgG, HRP conjugated, in 1 \times blocking buffer was added to each well and the plate was incubated at room temperature for 1 h with gentle shaking. After washing with 50 μL of PBS-T three times, chemiluminescence signal was developed by incubating each well with 20 μL of SuperSignal ELISA Pico Chemiluminescent Substrate at room temperature for 1 min with gentle shaking and the luminescent signal was recorded on a Infinite M1000 PRO instrument.

Native PAGE Analysis of Antibody–Ligand Complex. 5 μL of 50 $\mu\text{g}/\text{mL}$ anti-FLAG M2 mouse IgG (Sigma-Aldrich) was mixed with 2.5 μL of 0.12–7.4 μM FLAG-dextran or HA-dextran and incubated at RT for 1 h. The solution was mixed with 2.5 μL of NativePAGE Sample Buffer (Life Technologies), applied to NativePAGE Novex 3–12% Bis-Tris Gel (Life Technologies), and run at 150 V for 60 min then 250 V for 45 min at 4 $^{\circ}\text{C}$. The gel was fixed with 40% ethanol/10% acetic acid/50% ultrapure water and stained by using Pierce Silver Stain for Mass Spectrometry (Thermo Scientific).

SE-HPLC Analysis of Antibody–Ligand Complex. 0.5 μM of antibody was mixed with various concentrations of ligand-dextran in PBS buffer (pH 7.4) and incubated at RT for 30 min with rotation. After the incubation, 100 μL of the mixture was analyzed by SE-HPLC (TSKgel G4000SW_{XL}). Flow rate was 0.5 mL/min and UV absorbance was monitored at 220 nm.

SEC-MALS Analysis of FLAG-Dextran and a Complex Formed by FLAG-Dextran and anti-FLAG IgG1. SEC-MALS was performed using an HPLC (Agilent) with a size-exclusion column (WTC-030S5, Wyatt Technology) and 0.5 mL/min flow rate. For each sample, 100 μL solution was applied to the column. The eluent flowed through a UV detector (Agilent), a multiangle light scattering detector (Wyatt DAWN HELEOS II), and a refractive index detector (Wyatt Optilab T-rEX). Anti-FLAG IgG was diluted to 0.075 mg/mL and I-dextran was diluted to 0.25 mg/mL prior to injection to determine the molar mass distributions of each pure species. Anti-FLAG IgG and I-dextran were mixed to final concentrations of 0.075 and 0.025 mg/mL, respectively, to determine the molar mass distribution of the complexes formed. The light scattering and concentration data were analyzed by using ASTRA software (version 6.1, Wyatt).

Cell Binding Assay by Fluorescence Activated Cell Sorting (FACS). HEK 293 T cells were grown to 70% confluency 1 day after passage. Cells were transiently cotransfected with IgG light chain (pIg-lambda) and heavy chain (pIg-gamma-TM) plasmids using 293-fectin transfection reagents from Life Technologies following manufacturer's instructions. Cells were grown for 48 to 72 h at 37 $^{\circ}\text{C}$ in 5% CO_2 before collecting from the flask using enzyme-free cell dissociation buffer, washed with RPMI media, and resuspended in binding buffer (PBS containing 1% BSA and 0.1% sodium azide, pH 7.4). About 0.5×10^6 cells expressing CLL smlg (CLL 014, 068, 169 or 183) or untransfected HEK 293 T cells were aliquoted in each well of a 96-well microtiter plate. Cells were preblocked with 2% BSA in PBS containing 0.1% sodium azide and incubated with 16-biotin (50 nM), 17-biotin (50 nM), 16-dextran-biotin (25 nM), or 17-dextran-biotin (25 nM) for 45 min at 4 $^{\circ}\text{C}$ in PBS containing 1% BSA and 0.1% sodium azide for binding. Cells were washed five times with binding buffer, and treated with 1:50 dilution of streptavidin-phycoerythrin (saPE, from BD Bioscience) for 30 min on ice following 1:500 dilution of goat anti-human Fc-IgG conjugated

to allophycocyanine (anti-huFc-APC, from Jackson ImmunoResearch Laboratory Inc.) for 30 min on ice. Following washing three times with binding buffer, the expression of smlg on cells was detected by APC signal and the binding was detected by PE signal on fluorescence activated cell sorting (BD FACSCanto II).

■ ASSOCIATED CONTENT

📄 Supporting Information

Figure S1–S7 and Table S1. This material is available free of charge via the Internet at <http://pubs.acs.org>.

■ AUTHOR INFORMATION

Corresponding Author

*E-mail: Kodadek@scripps.edu.

Notes

The authors declare no competing financial interest.

■ ACKNOWLEDGMENTS

This study was funded by a grant from the NIH (DP3 DK094309) and a contract from the NHLBI (NO1-HV-00242). J. M. was supported by the JSPS Postdoctoral Fellowship for Research Abroad program. We thank Wyatt Technology for the MALS measurement of the dextran-conjugate, Dr. Jeffrey L. Bennett (University of Colorado) for providing monoclonal, patient-derived anti-AQP4 IgG1, Dr. Michael Levy for providing serum samples from NMO patients, and Dr. Nicholas Chiorazzi for the CLL 169 antibody-expressing plasmids. We also thank Drs. Tina Izard and Rangarajan Erumbi of The Scripps Research Institute and Dr. Sophia Kenrick of Wyatt technology for useful discussions regarding MALS analyses.

■ REFERENCES

- (1) Matthews, R. (2007) The B cell slayer. *Science* 318, 1232–1233.
- (2) Duxbury, B., Combesure, C., and Chizzolini, C. (2013) Rituximab in systemic lupus erythematosus: an updated systematic review and meta-analysis. *Lupus* 22, 1489–503.
- (3) Hauser, S. L., Waubant, E., Arnold, D. L., Vollmer, T., Antel, J., Fox, R. J., Bar-Or, A., Panzara, M., Sankar, N., Agarwal, S., Langer-Gould, A., and Smith, C. H. (2008) B-cell depletion with rituximab in relapsing-remitting multiple sclerosis. *N. Engl. J. Med.* 358, 676–88.
- (4) Furman, R. R., Sharman, J. P., Coutre, S. E., Cheson, B. D., Pagel, J. M., Hillmen, P., Barrientos, J. C., Zelenetz, A. D., Kipps, T. J., Flinn, I., Ghia, P., Eradat, H., Ervin, T., Lamanna, N., Coiffier, B., Pettitt, A. R., Ma, S., Stilgenbauer, S., Cramer, P., Aiello, M., Johnson, D. M., Miller, L. L., Li, D., Jahn, T. M., Dansey, R. D., Hallek, M., and O'Brien, S. M. (2014) Idelalisib and rituximab in relapsed chronic lymphocytic leukemia. *N. Engl. J. Med.* 370, 997–1007.
- (5) Wolchok, J. D., Hodi, F. S., Weber, J. S., Allison, J. P., Urba, W. J., Robert, C., O'Day, S. J., Hoos, A., Humphrey, R., Berman, D. M., Lonberg, N., and Korman, A. J. (2013) Development of ipilimumab: a novel immunotherapeutic approach for the treatment of advanced melanoma. *Ann. N.Y. Acad. Sci.* 1291, 1–13.
- (6) Azad, A., and Campbell, P. (2009) High rates of infection associated with the use of maintenance rituximab monotherapy in non-Hodgkin lymphoma. *Intern. Med. J.* 39, 778–9.
- (7) Lin, P. C., Hsiao, L. T., Poh, S. B., Wang, W. S., Yen, C. C., Chao, T. C., Liu, J. H., Chiou, T. J., and Chen, P. M. (2007) Higher fungal infection rate in elderly patients (more than 80 years old) suffering from diffuse large B cell lymphoma and treated with rituximab plus CHOP. *Ann. Hematol.* 86, 95–100.
- (8) Pырpаsοpουlου, Α., Dουmα, S., Vαssilιαdιs, T., Chαtzimιchαilidου, S., Triantafυllου, Α., and Αslανidιs, S. (2011) Reactivation of chronic

hepatitis B virus infection following rituximab administration for rheumatoid arthritis. *Rheumatol. Int.* 31, 403–4.

(9) Fecher, L. A., Agarwala, S. S., Hodi, F. S., and Weber, J. S. (2013) Ipilimumab and its toxicities: a multidisciplinary approach. *Oncologist* 18, 733–43.

(10) Chiorazzi, N., Rai, K. R., and Ferrarini, M. (2005) Chronic lymphocytic leukemia. *N. Engl. J. Med.* 352, 804–15.

(11) Jaglowski, S. M., Alinari, L., Lapalombella, R., Muthusamy, N., and Byrd, J. C. (2010) The clinical application of monoclonal antibodies in chronic lymphocytic leukemia. *Blood* 116, 3705–14.

(12) Reddy, M. M., Wilson, R., Wilson, J., Connell, S., Gocke, A., Hynan, L., German, D., and Kodadek, T. (2011) Identification of candidate IgG biomarkers for Alzheimer's Disease via combinatorial library screening. *Cell* 144, 132–142.

(13) Raveendra, B., Hao, W., Baccala, R., Reddy, M. M., Schilke, J., Bennett, J. L., Theofilopoulos, A. N., and Kodadek, T. (2013) Discovery of peptoid ligands for anti-Aquaporin 4 antibodies. *Chem. Biol.* 20, 350–359.

(14) Doran, T. M., Gao, Y., Mendes, K., Dean, S., Simanski, S., Kodadek, T. (2014) The utility of redundant combinatorial libraries in distinguishing high and low quality screening hits. *ACS Comb. Sci.* 16, In press.

(15) Wu, Y., Zhang, Q., Sales, D., Bianco, A. E., and Craig, A. (2010) Vaccination with peptide mimotopes produces antibodies recognizing bacterial capsular polysaccharides. *Vaccine* 28, 6425–35.

(16) Kozbor, D. (2010) Cancer vaccine with mimotopes of tumor-associated carbohydrate antigens. *Immunol. Res.* 46, 23–31.

(17) Knittelfelder, R., Riemer, A. B., and Jensen-Jarolim, E. (2009) Mimotope vaccination—from allergy to cancer. *Expert Opin. Biol. Ther.* 9, 493–506.

(18) Seiler, T., Woelfle, M., Yancopoulos, S., CATERA, R., Li, W., Hatzl, K., Moreno, C., Torres, M., Paul, S., Dohner, H., Stilgenbauer, S., Kaufman, M. S., Kolitz, J. E., Allen, S. L., Rai, K. R., Chu, C. C., and Chiorazzi, N. (2009) Characterization of structurally defined epitopes recognized by monoclonal antibodies produced by chronic lymphocytic leukemia B cells. *Blood* 114, 3615–24.

(19) Gocke, A. R., Udagamasooriya, D. G., Archer, C. T., Lee, J., and Kodadek, T. (2009) Isolation of antagonists of antigen-specific autoimmune T cell proliferation. *Chem. Biol.* 16, 1133–9.

(20) Gao, Y., and Kodadek, T. (2013) Synthesis and screening of stereochemically diverse combinatorial libraries of peptide tertiary amides. *Chem. Biol.* 20, 360–369.

(21) Aquino, C., Sarkar, M., CHalmers, M. J., Mendes, K., Kodadek, T., and Micalizio, G. (2011) A biomimetic polyketide-inspired approach to small molecule ligand discovery. *Nat. Chem.* 4, 99–104.

(22) Kiessling, L. L., Gestwicki, J. E., and LE, S. (2000) Synthetic multivalent ligands in the exploration of cell-surface interactions. *Curr. Opin. Chem. Biol.* 4, 696–703.

(23) Schweitzer-Stenner, R., Licht, A., Luscher, I., and Pecht, I. (1987) Oligomerization and ring closure of immunoglobulin E class antibodies by divalent haptens. *Biochemistry* 26, 3602–12.

(24) Baird, E. J., Holowka, D., Coates, G. W., and Baird, B. (2003) Highly effective poly(ethylene glycol) architectures for specific inhibition of immune receptor activation. *Biochemistry* 42, 12739–48.

(25) Mack, E. T., Snyder, P. W., Perez-Castillejos, R., and Whitesides, G. M. (2011) Using covalent dimers of human carbonic anhydrase II to model bivalency in immunoglobulins. *J. Am. Chem. Soc.* 133, 11701–15.

(26) Das, R., Baird, E., Allen, S., Baird, B., Holowka, D., and Goldstein, B. (2008) Binding mechanisms of PEGylated ligands reveal multiple effects of the PEG scaffold. *Biochemistry* 47, 1017–30.

(27) Rostovtsev, V. V., Green, L. G., Fokin, V. V., and Sharpless, K. B. (2002) A stepwise Huisgen cycloaddition process: copper(I)-catalyzed regioselective "ligation" of azides and terminal alkynes. *Angew. Chem., Int. Ed.* 41, 2596–9.

(28) Luedtke, R., Owen, C. S., and Karush, F. (1980) Proximity of antibody binding sites studied by fluorescence energy transfer. *Biochemistry* 19, 1182–92.

(29) Saphire, E. O., Stanfield, R. L., Crispin, M. D., Parren, P. W., Rudd, P. M., Dwek, R. A., Burton, D. R., and Wilson, I. A. (2002) Contrasting IgG structures reveal extreme asymmetry and flexibility. *J. Mol. Biol.* 319, 9–18.

(30) Lennon, V. A., Wingerchuk, D. M., Kryzer, T. J., Pittock, S. J., Lucchinetti, C. F., Fujihara, K., Nakashima, I., and Weinshenker, B. G. (2004) A serum autoantibody marker of neuromyelitis optica: distinction from multiple sclerosis. *Lancet* 364, 2106–12.

(31) Lennon, V. A., Kryzer, T. J., Pittock, S. J., Verkman, A. S., and Hinson, S. R. (2005) IgG marker of optic-spinal multiple sclerosis binds to the aquaporin-4 water channel. *J. Exp. Med.* 202, 473–7.

(32) Bennett, J. L., Lam, C., Kalluri, S. R., Saikali, P., Bautista, K., Dupree, C., Glogowska, M., Case, D., Antel, J. P., Owens, G. P., Gilden, D., Nessler, S., Stadelmann, C., and Hemmer, B. (2009) Intrathecal pathogenic anti-aquaporin-4 antibodies in early neuromyelitis optica. *Ann. Neurol.* 66, 617–29.

(33) Doran, T. M., and Kodadek, T. (2013) A liquid array platform for the multiplexed analysis of synthetic molecule-protein interactions. *ACS Chem. Biol.* 9, 339–346.

(34) van Cleve, J. W., Schaefer, W. C., and Rist, C. E. (1956) The structure of NRRL B-512 dextran. Methylation studies. *J. Am. Chem. Soc.* 78, 4435–4438.

(35) Nakamura, J., Nakajima, N., Matsumura, K., and Hyon, S. H. (2010) Water-soluble taxol conjugates with dextran and targets tumor cells by folic acid immobilization. *Anticancer Res.* 30, 903–9.

(36) Rief, M., Oesterhelt, F., Heymann, B., and Gaub, H. E. (1997) Single molecule force spectroscopy on polysaccharides by atomic force microscopy. *Science* 275, 1295–7.

(37) Liu, Y., Higgins, C. D., Overstreet, C. M., Rai, K. R., Chiorazzi, N., and Lai, J. R. (2013) Peptides that bind specifically to an antibody from a chronic lymphocytic leukemia clone expressing unmutated immunoglobulin variable region genes. *Mol. Med.* 19, 245–52.

(38) Nangreave, J., Yan, H., and Liu, Y. (2011) DNA nanostructures as models for evaluating the role of enthalpy and entropy in polyvalent binding. *J. Am. Chem. Soc.* 133, 4490–4497.

(39) Baird, B., Zheng, Y., and Holowka, D. (1993) Structural mapping of Ige-Fc-epsilon-Ri, an immunoreceptor complex. *Acc. Chem. Res.* 26, 428–434.

(40) Warr, G. W., Magor, K. E., and Higgins, D. A. (1995) IgY: clues to the origins of modern antibodies. *Immunol. Today* 16, 392–8.

(41) Janssen, B. M. G., Lempens, E. H. M., Olijve, L. L. C., Voets, I. K., van Dongen, J. L. J., de Greef, T. F. A., and Merckx, M. (2013) Reversible blocking of antibodies using bivalent peptide-DNA conjugates allows protease-activatable targeting. *Chem. Sci.* 4, 1442–1450.

(42) Figliozzi, G. M., Goldsmith, R., Ng, S. C., Banville, S. C., and Zuckermann, R. N. (1996) Synthesis of N-substituted glycine peptoid libraries. *Methods Enzymol.* 267, 437–447.

(43) Habeeb, A. F. (1966) Determination of free amino groups in proteins by trinitrobenzenesulfonic acid. *Anal. Biochem.* 14, 328–36.